

Structural bioinformatics

# A natural upper bound to the accuracy of predicting protein stability changes upon mutations

Ludovica Montanucci<sup>1,†</sup>, Pier Luigi Martelli<sup>2,†</sup>, Nir Ben-Tal<sup>3,\*</sup> and Piero Fariselli <sup>1,\*</sup>

<sup>1</sup>Department of Comparative Biomedicine and Food Science, University of Padova, Legnaro 35020, Italy, <sup>2</sup>Biocomputing Group, Department of Pharmacy and Biotechnology, University of Bologna, Bologna 40126, Italy and <sup>3</sup>Department of Biochemistry and Molecular Biology, George S. Wise Faculty of Life Sciences, Tel Aviv University, Tel Aviv 69978, Israel

\*To whom correspondence should be addressed.

<sup>†</sup>The authors wish it to be known that, in their opinion, the first two authors should be regarded as Joint First Authors.

Associate Editor: Alfonso Valencia

Received on June 8, 2018; revised on September 7, 2018; editorial decision on October 11, 2018; accepted on October 16, 2018

## Abstract

**Motivation:** Accurate prediction of protein stability changes upon single-site variations ( $\Delta\Delta G$ ) is important for protein design, as well as for our understanding of the mechanisms of genetic diseases. The performance of high-throughput computational methods to this end is evaluated mostly based on the Pearson correlation coefficient between predicted and observed data, assuming that the upper bound would be 1 (perfect correlation). However, the performance of these predictors can be limited by the distribution and noise of the experimental data. Here we estimate, for the first time, a theoretical upper-bound to the  $\Delta\Delta G$  prediction performances imposed by the intrinsic structure of currently available  $\Delta\Delta G$  data.

**Results:** Given a set of measured  $\Delta\Delta G$  protein variations, the theoretically “best predictor” is estimated based on its similarity to another set of experimentally determined  $\Delta\Delta G$  values. We investigate the correlation between pairs of measured  $\Delta\Delta G$  variations, where one is used as a predictor for the other. We analytically derive an upper bound to the Pearson correlation as a function of the noise and distribution of the  $\Delta\Delta G$  data. We also evaluate the available datasets to highlight the effect of the noise in conjunction with  $\Delta\Delta G$  distribution. We conclude that the upper bound is a function of both uncertainty and spread of the  $\Delta\Delta G$  values, and that with current data the best performance should be between 0.7 and 0.8, depending on the dataset used; higher Pearson correlations might be indicative of overtraining. It also follows that comparisons of predictors using different datasets are inherently misleading.

**Contact:** bental@tauex.tau.ac.il or piero.fariselli@unipd.it

**Supplementary information:** [Supplementary data](#) are available at *Bioinformatics* online.

## 1 Introduction

Prediction of protein stability changes upon mutation is a crucial step in the understanding of protein function in health and disease, and may facilitate protein design. Several computational methods have been developed to predict the direction (stabilizing vs. destabilizing), and the magnitude of the perturbation of the stability of a protein

introduced by a single-point mutation in its sequence (Capriotti *et al.*, 2005, 2008; Chen *et al.*, 2013; Cheng *et al.*, 2006; Fariselli *et al.*, 2015; Folkman *et al.*, 2016; Giollo *et al.*, 2014; Huang *et al.*, 2007; Laimer *et al.*, 2016; Masso and Vaisman, 2008; Parthiban *et al.*, 2006; Pires *et al.*, 2014a,b; Pucci *et al.*, 2017; Savojardo *et al.*, 2016; Teng *et al.*, 2010; Topham *et al.*, 1997; Wainreb *et al.*, 2011;

Worth *et al.*, 2011; Yin *et al.*, 2007; Zhou and Zhou, 2002). Most of these methods are based on machine learning, and, at state of the art, their Pearson correlation performances range from 0.5–0.8.

The development of prediction methods has been made possible by compilations of datasets of experimentally measured changes in protein stability upon single-point variations [ $\Delta\Delta G = \Delta G_{\text{wildtype}} - \Delta G_{\text{mutant}}$ , the folding free energy difference between the wildtype and mutant protein; (Broom *et al.*, 2017; Dehouck *et al.*, 2011; Guerois *et al.*, 2002; Kumar *et al.*, 2006; Pires *et al.*, 2014)]. Among these, ProTherm (Kumar *et al.*, 2006) is the most comprehensive dataset, aiming at collecting from primary literature all the experimentally determined thermodynamic values for calorimetry experiments in protein and protein mutants and making them available in a unified format. Therefore, data collected in ProTherm come from experiments performed with different techniques and in different environmental conditions. Each experimental condition is defined by several characteristics, such as pH, temperature, additives in the solution, salt concentration, ion concentration, protein concentration, the concentration of the denaturant, addition of peptides to the protein sequence, etc.

Different environmental conditions, such as pH and temperature, yield different  $\Delta\Delta G$  values. In Keeler *et al.* (2009), the stability change of variation H180A in the human prolactin (2Q98) was measured at the same temperature (25°C) but in two different pH conditions: pH = 5.8 and pH = 7.8. The corresponding  $\Delta\Delta G$  values are 1.39 kcal/mol and -0.04 kcal/mol, respectively. Even when the temperature and pH are the same, two measures of  $\Delta\Delta G$  can differ due to other experimental conditions or different techniques. This is the case for the E3R variation in protein 1CSP, for which six different  $\Delta\Delta G$  values ranging from 1.4 kcal/mol to 2.4 kcal/mol were measured (Gribenko and Makhatadze, 2007) at the same temperature (55°C) and pH (7.5) but at six different salt concentrations ranging from 0 to 1.0 M NaCl. In Ferguson and Shaw (2002) the variant L3S of the calcium-binding protein S100B (1UWO) measured in two different conditions but at the same temperature (25°C) and pH (7.2) yielded two  $\Delta\Delta G$  values of 1.91 kcal/mol and -2.77 kcal/mol. Here not only the value of the  $\Delta\Delta G$  changes, but also the sign, i.e., whether the mutation is stabilizing or destabilizing.

The broad range of experimental conditions in which  $\Delta\Delta G$  are measured increases the actual uncertainty associated with them in the databases. In other words, the error of a wet-lab experimental determination of a  $\Delta\Delta G$  in a single experiment can be quite small, roughly ranging from 0.1 to 0.5 kcal/mol [as an example it is 0.14 kcal/mol for thermal unfolding in Perl and Schmid (2001) and as small as 0.06 and 0.09 kcal/mol in De Prat Gay *et al.* (1994)]. Nonetheless, the experimental conditions in which the  $\Delta\Delta G$  measures are carried out can vary substantially, introducing other sources of uncertainty associated with the measurements.

Given that all prediction methods exploit these data, an estimate of the theoretical upper bound for the prediction is crucial for the understanding and interpretation of the results. Here we approximate this upper bound by deriving an analytical expression, and by analyzing the experimental data. We show that the best performance depends on the dataset used, and would typically be significantly lower than expected.

## 2 Theoretical estimation

### 2.1 Data uncertainty and representation of the data with a probabilistic model

Given the broad range of values that the parameters of the experimental conditions can assume, the uncertainty associated with each  $\Delta\Delta G$  measurement for a set of single-point variations is greater than

the actual experimental error of 0.1–0.5 kcal/mol (because it includes effects due to changes in experimental conditions). This uncertainty, indicated here as  $\sigma$ , can differ from one case to another.

A set of experiments performed on  $N$  different protein variations produce  $N$  observed  $\Delta\Delta G$  values indicated here as  $\{x_i\}$ . In the limit of the uncertainty  $\sigma$  approaching 0, the value of  $x_i$  tends to the “real”  $\Delta\Delta G$  value for each variation. Our hypothesis here is that repeated observations  $x_i$  for the same variation  $i$  are distributed around the real  $i$ -th  $\Delta\Delta G$  value and have a standard deviation equal to the (unknown) uncertainty  $\sigma_i$ . We do not pose restrictions on the nature of the data distribution. We indicate with  $\mu_i$  the real  $\Delta\Delta G$  value of a variation, determined in the wet-lab at arbitrary precision (for which all the conditions are enumerated and measured).

A set of  $N$  experimentally observed  $\Delta\Delta G$  values  $\{x_i\}$  can be generated by choosing each  $x_i$  with probability given by its specific distribution  $P_i(x_i) = P_i(x_i|\mu_i, \sigma_i)$  with mean given by the  $i$ -th real  $\Delta\Delta G$  value  $\mu_i$  and with standard deviation given by the unknown uncertainty  $\sigma_i$ .

### 2.2 Theoretical correlation between two observed distributions as a function of the variances

We consider a sufficiently large number of samples to estimate the correlation between two sets of observations and hence establish a general analytical expression for the correlation between them. This is particularly useful if we want to use a set of observed  $\Delta\Delta G$  values  $\{x_i\}$  as predictors for another set of observed  $\Delta\Delta G$  values  $\{y_i\}$ . Because we assume that no computational method can predict better than another set of experiments conducted in similar conditions, this correlation represents an upper bound for the correlation that any predictor that uses  $\{x_i\}$  as a training set can achieve. Our goal is to estimate the correlation between a pair of sets of experimental observations,  $\{x_i\}$  and  $\{y_i\}$ , of the same set of variations with real  $\Delta\Delta G$  values equal to  $\{\mu_i\}$ . We assume that both  $\{x_i\}$  and  $\{y_i\}$  are derived from the same set of distributions ( $P_i(x_i) = P_i(x_i|\mu_i, \sigma_i) = P_i(y_i) = P_i(y_i|\mu_i, \sigma_i)$ ), where the distributions  $P_i$  can differ for each protein variation  $i$ . In the following, we only assume that the means and variances are finite, with common definitions

$$\begin{aligned}\mu_i &= \langle y_i \rangle = \langle x_i \rangle = \int_{-\infty}^{\infty} x_i P_i(x_i) dx_i \\ \sigma_i^2 &= \langle (y_i - \mu_i)^2 \rangle = \langle (x_i - \mu_i)^2 \rangle = \int_{-\infty}^{\infty} (x_i - \mu_i)^2 P_i(x_i) dx_i\end{aligned}\quad (1)$$

where the angular brackets represent expected values. With this notation, the expectation of the Pearson correlation is defined as:

$$\langle \rho \rangle = \left\langle \frac{\sigma_{xy}}{\sigma_x \sigma_y} \right\rangle \quad (2)$$

Considering a sufficiently large number of samples, we can set  $\sigma_x \cong \sigma_y$ , since they are computed in the same way from the same distributions. The Pearson denominator simplifies as  $\sigma_x \sigma_y \cong \sigma_x^2 \cong \sigma_y^2$  (which is the variance of one of the two variables). To work out an analytical solution, instead of computing the expectation of the Pearson directly, we compute the ratio of the expectations of the numerator and denominators. In general, this is correct only to the first order, however, when the number of samples is sufficiently large, the Pearson correlation  $\rho$  is independent of the variance  $\sigma_x^2$ , so that the covariance between them is zero ( $\text{Cov}(\rho, \sigma_x^2) \cong 0$ ). We can see this by generating an infinite set of different variance values by scaling the original variables ( $x'_i = k \cdot x_i$  and  $y'_i = k \cdot y_i$ ), while

maintaining the same Pearson value  $\rho$ . Since it is possible to write the covariance as a function of expectations (Heijmans, 1999) as

$$\text{Cov}(\rho, \sigma_x^2) = \langle \sigma_{xy} \rangle - \langle \rho \rangle \langle \sigma_x^2 \rangle \quad (3)$$

from the independence of Pearson and variance ( $\text{Cov}(\rho, \sigma_x^2) \cong 0$ ) it follows that the expected value of the Pearson correlation can be approximated as

$$\langle \rho \rangle \cong \langle \sigma_{xy} \rangle / \langle \sigma_x^2 \rangle \quad (4)$$

The numerator in Equation (4) can be computed by taking the expected values of the variables  $\{x_i\}$  and  $\{y_i\}$ , as:

$$\begin{aligned} \langle \sigma_{xy} \rangle &= \left\langle \frac{1}{N} \sum_i (x_i - \bar{x})(y_i - \bar{y}) \right\rangle \\ &= \frac{1}{N} \sum_i \int (x_i - \bar{x}) P_i(x_i) dx_i \int (y_i - \bar{y}) P_i(y_i) dy_i \end{aligned} \quad (5)$$

where  $\bar{x}$  and  $\bar{y}$  are the mean values of variables  $\{x_i\}$  and  $\{y_i\}$ . The first term in the arguments of the two integrals can be expanded by adding and subtracting the same value, in this case we choose to add and subtract the real value for the distributions:  $\mu_i$ . Hence, the argument of the first integral  $(x_i - \bar{x})$  can be expanded as  $(x_i - \mu_i) + (\mu_i - \bar{x})$ . Similarly, in the second integral,  $(y_i - \bar{y})$  can be expanded as  $(y_i - \mu_i) + (\mu_i - \bar{y})$ . The resulting formula becomes:

$$\begin{aligned} \langle \sigma_{xy} \rangle &= \frac{1}{N} \sum_i \left[ \left( \int (x_i - \mu_i) P_i(x_i) dx_i + \int (\mu_i - \bar{x}) P_i(x_i) dx_i \right) \right. \\ &\quad \left. \left( \int (y_i - \mu_i) P_i(y_i) dy_i + \int (\mu_i - \bar{y}) P_i(y_i) dy_i \right) \right] \end{aligned} \quad (6)$$

We notice that the first and third integrals go to zero (as  $N$  increases), by definition of the mean, Equation (1), while the second and fourth integrals, after taking out the terms that do not depend on the integration variable, give 1 (for the normalization of the distribution  $P_i$ ). So the numerator becomes:

$$\begin{aligned} \frac{1}{N} \sum_i \left( \int (\mu_i - \bar{x}) P_i(x_i) dx_i \right) \left( \int (\mu_i - \bar{y}) P_i(y_i) dy_i \right) \\ = \frac{1}{N} \sum_i (\mu_i - \bar{x})(\mu_i - \bar{y}) \end{aligned} \quad (7)$$

Assuming that the two experimental sets are derived from the same distribution, with an average of  $\bar{\mu}$  (which would be the case unless there are systematic errors),  $\bar{x}$  and  $\bar{y}$  would equal  $\bar{\mu}$ , and the numerator in Equation (4) would tend to:

$$\sigma_{DB}^2 = \frac{1}{N} \sum_i (\mu_i - \bar{\mu})^2 \quad (8)$$

This is the variance of the distribution of the real  $\Delta\Delta G$  values, which does not depend on the experimental uncertainty but only on the distribution of the  $\Delta\Delta G$  values in our database (hence  $\sigma_{DB}$ ). The database distribution can be of any type, the only value we consider is its variance  $\sigma_{DB}^2$ . So we can estimate the covariance as:

$$\langle \sigma_{xy} \rangle \cong \sigma_{DB}^2 \quad (9)$$

For the denominator of the Pearson correlation [Equation (4)] we have:

$$\sigma_x^2 = \frac{1}{N} \sum_i (x_i - \bar{x})^2 \quad (10)$$

We can estimate the variance as before, thus for  $\sigma_x^2$  we obtain:

$$\begin{aligned} \langle \sigma_x^2 \rangle &= \left\langle \frac{1}{N} \sum_i (x_i - \bar{x})^2 \right\rangle = \frac{1}{N} \sum_i \int (x_i - \bar{x})^2 P_i(x_i) dx_i \\ &= \frac{1}{N} \sum_i \int [(x_i - \mu_i) + (\mu_i - \bar{x})]^2 P_i(x_i) dx_i \\ &= \frac{1}{N} \sum_i \int [(x_i - \mu_i)^2 + (\mu_i - \bar{x})^2 + 2(x_i - \mu_i)(\mu_i - \bar{x})] P_i(x_i) dx_i \end{aligned} \quad (11)$$

When integrated, the last term of the integral goes to zero as  $N$  increases [based on the definition of mean, Equation (1)], while the first and the second approach the uncertainty  $\sigma_i^2$  associated with each  $\Delta\Delta G$  point, and  $\sigma_{DB}^2$  of the real data set, respectively. Thus, the variance can be estimated as:

$$\langle \sigma_x^2 \rangle \cong \bar{\sigma}^2 + \sigma_{DB}^2 \quad (12)$$

Where we indicate with  $\bar{\sigma}^2$  the average variance of the data

$$\bar{\sigma}^2 = \frac{1}{N} \sum_i \sigma_i^2 \quad (13)$$

and with  $\bar{\sigma}$  its square root ( $\bar{\sigma} = \sqrt{\bar{\sigma}^2}$ ). With this, the Pearson correlation [Equation (4)] can be estimated as:

$$\langle \rho \rangle \cong \frac{\langle \sigma_{xy} \rangle}{\langle \sigma_x^2 \rangle} \cong \frac{\sigma_{DB}^2}{\bar{\sigma}^2 + \sigma_{DB}^2} = \frac{1}{1 + \left( \frac{\bar{\sigma}^2}{\sigma_{DB}^2} \right)} \quad (14)$$

Given that the two variances are greater than zero, the experimental observations will always yield Pearson correlation smaller than 1. The magnitude of the reduction of the correlation is imposed by the squared ratio of the average uncertainty of each data point ( $\Delta\Delta G$  value) and the spread of the set of data used for the prediction. Equation (14) indicates that the smaller the dispersion of the dataset  $\sigma_{DB}^2$ , the more sensitive the Pearson correlation is to the data noise (or uncertainty,  $\bar{\sigma}$ ). In other words, two datasets that share the same average uncertainty but differ in their data distribution have different upper bound Pearson correlations.

Figure 1 shows a graphical plot of the correlation  $\rho$  as a function of the average uncertainty  $\bar{\sigma}$  and the standard deviation  $\sigma_{DB}$ . Each curve represents the upper bound that a Pearson correlation can achieve. For example, with  $\sigma_{DB}$  of 2 kcal/mol and average uncertainty  $\bar{\sigma}$  of 1 kcal/mol, the maximum Pearson correlation that any predictor can achieve is only about 0.8.

### 3 Experimental datasets

To be more realistic, we supplement the approximate theoretical derivation of Section 2 with estimates based on real mutation data taken from the available databases.

#### 3.1 Distribution of the available data

We considered three datasets used to train most of the available computational methods. The first is the latest version of ProTherm (Kumar *et al.*, 2006, last update in 2013) comprising 3464 single-point mutations from 135 proteins of known structure (with PDB IDs). The second is S2648 (Dehouck *et al.*, 2011) which comprises 2648 single-site variations in 131 proteins taken and cleaned from a previous release of ProTherm. The third is VariBench, a manually curated dataset, for which the  $\Delta\Delta G$  measurements have been

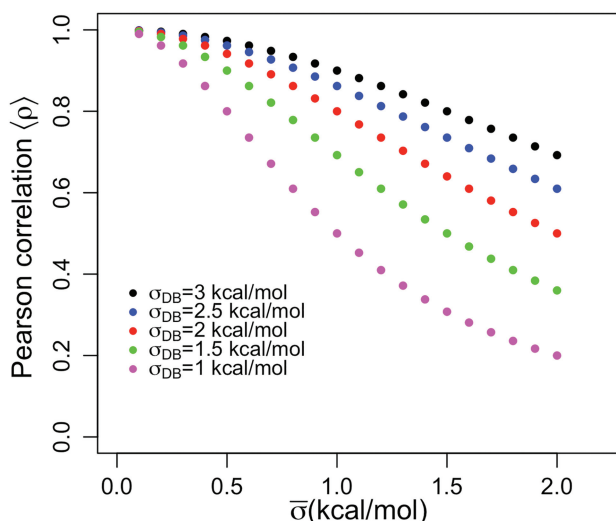


**Fig. 1.** Expected Pearson correlation  $\langle \rho \rangle$  vs. data average uncertainty ( $\bar{\sigma}$ ) for different values of dataset standard deviation  $\sigma_{DB}$ . The results were calculated using the approximate analytical expression of Equation (14), with each curve corresponding to a specific  $\sigma_{DB}$ . The ratio between  $\bar{\sigma}$  and  $\sigma_{DB}$  determines the approximate upper bound of  $\rho$ , which, for finite values of these uncertainties, will always be smaller than 1

checked in the primary literature. VariBench (Yang et al., 2018) is derived from the ProTherm release of February 22, 2013 and contains 1564 single-site variations from 99 proteins.

The three datasets have a very sharp distribution around the average value (around  $-1.06$  kcal/mol for each set), with low standard deviations ( $\sigma_{DB}$ ) of 2.06 kcal/mol in ProTherm, 1.91 kcal/mol in VariBench, and 1.47 kcal/mol in S2648 (Supplementary Fig. S1). The theoretical model above [Equation (14)] shows that with such low deviations, the Pearson correlation should be sensitive to noise.

It is also noteworthy that because of the difference in their standard deviations, the maximum possible Pearson correlation of the three datasets, for the same average experimental uncertainty  $\bar{\sigma}$ , is not the same. In particular, if both the VariBench and S2648 datasets are affected by the same average experimental uncertainty  $\bar{\sigma}$ , the maximum possible Pearson correlation of VariBench would be larger.

### 3.2 What can we expect from the current experimental datasets?

We made a raw evaluation of what we can expect from the current experimental dataset. In particular, we considered two datasets:

1. S1: a subset of 574 ProTherm single-site variations for which two or more experimental  $\Delta\Delta G$  values are reported for the same protein variation, measured at the same temperature and pH;
2. S2: a subset of 551 variations shared by VariBench and S2648, for which the manual curators ended up with different  $\Delta\Delta G$  values.

Thus, for each variation  $i$  (in either S1 and S2), we can associate a mean value ( $\mu_i = \Delta\Delta G_i$ ) and a standard deviation ( $\sigma_i$ ), since we have at least two  $\Delta\Delta G$  values. Computing  $\bar{\sigma}$  (as the square root of the mean of  $\{\sigma_i^2\}$ ) and the  $\sigma_{DB}$  (using the  $\{\Delta\Delta G_i\}$ ) for S1 and S2, we obtained  $\bar{\sigma}=1.04$  and  $\sigma_{DB}=1.72$ , and  $\bar{\sigma}=0.72$  and  $\sigma_{DB}=1.57$ , respectively. Substituting these values in Equation (14), we obtain estimations of maximum Pearson correlations of 0.73 for S1 and 0.83 for S2. However, the same data can be used to explicitly take into account the different  $\{\sigma_i^2\}$  values. For each variation it is possible to

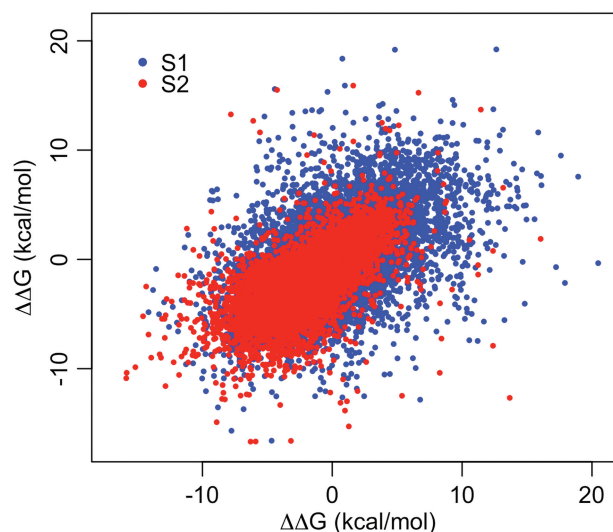


**Fig. 2.** Scatterplot of two randomly generated observations for a given variation. Red points are 100 randomly generated observations according to a normal distribution, with  $\overline{\Delta\Delta G}_i$  and  $\sigma_i$  taken from the manually curated S2: different value for the same mutation reported in S2648 and VeriBench). Blue points are 100 randomly generated observations according to a normal distribution with  $\overline{\Delta\Delta G}_i$  and  $\sigma_i$  taken from S1: ProTherm variations with more than one  $\Delta\Delta G$  value reported for the same variation at the same pH and temperature

derive a set of pairs of “experiments” by randomly drawing two values at a time from the normal distribution  $N(\overline{\Delta\Delta G}_i, \sigma_i)$ . Figure 2 shows the results of a typical run. By drawing 100 pairs of such “experiments”, and repeating the runs 10 times, we obtained an estimation of the Pearson correlation (with variable  $\{\sigma_i\}$ ) of  $0.74 \pm 0.02$  and  $0.84 \pm 0.02$ , for S1 and S2 respectively.

## 4 Conclusion

Using a general model we approximated the correlation between a pair of observed  $\Delta\Delta G$  measurements, where one is used to predict the other. An approximate analytical expression, as well as simulations using real data, show that the correlation is limited by the ratio between these two uncertainties, placing a natural upper bound on the maximum possible Pearson correlation between predicted and empirical values. With current accuracy, the theoretical value critically depends on both the average uncertainty of the data ( $\bar{\sigma}$ ) and the spread of the dataset used ( $\sigma_{DB}$ ). While the first can be reduced to some extent by manually cleaning the data,  $\sigma_{DB}$  is an intrinsic property of the dataset that provides an upper bound to the maximum expected Pearson correlation.

A similar approach can be used to derive a lower bound for the root mean square error (Rmse), another commonly used measure of performance. In Supplementary Material we show that the expected value of the root mean square error is a linear function of the average data uncertainty ( $\langle Rmse \rangle \cong \sqrt{2}\bar{\sigma}$ ). The current datasets (S2648, VariBench) have a  $\sigma_{DB} < 2$ , dictating an upper bound of about 0.8 to the Pearson correlation and lower bound of about 1 kcal/mol for the root mean square error (see Supplementary Material); better values would be indicative of overtraining.

Generally speaking, the conclusions should be valid whenever large empirical datasets compiled of various measurements are used for training a predictor, and Equation (14) gives an approximate upper bound for the prediction accuracy.

## Funding

This work was supported by EBA-PRISM an Israel-Italy collaborative project, the Israel Ministry of Science and Technology and Italian Ministry of Foreign Affairs and International Cooperation. NB-T's research is supported in part by the Abraham E. Kazan Chair in Structural Biology, Tel Aviv University.

*Conflict of Interest:* none declared.

## References

- Broom, A. *et al.* (2017) Computational tools help improve protein stability but with a solubility tradeoff. *J. Biol. Chem.*, **292**, 14349–14361.
- Capriotti, E. *et al.* (2005) I-Mutant2.0: predicting stability changes upon mutation from the protein sequence or structure. *Nucleic Acids Res.*, **33**, 306–310.
- Capriotti, E. *et al.* (2008) A three-state prediction of single point mutations on protein stability changes. *BMC Bioinformatics*, **9**, S6.
- Chen, C.W. *et al.* (2013) iStable: off-the-shelf predictor integration for predicting protein stability changes. *BMC Bioinformatics*, **14**, S5.
- Cheng, J. *et al.* (2006) Prediction of protein stability changes for single-site mutations using support vector machines. *Proteins*, **62**, 1125–1132.
- De Prat Gay, G. *et al.* (1994) Contribution of a proline residue and a salt bridge to the stability of a type I reverse turn in chymotrypsin inhibitor-2. *Protein Eng.*, **7**, 103–108.
- Dehouck, Y. *et al.* (2011) PoPMuSiC 2.1: a web server for the estimation of protein stability changes upon mutation and sequence optimality. *BMC Bioinformatics*, **12**, 151.
- Fariselli, P. *et al.* (2015) INPS: predicting the impact of non-synonymous variations on protein stability from sequence. *Bioinformatics*, **31**, 2816–2821.
- Ferguson, P.L., and Shaw, G.S. (2002) Role of the N-terminal helix I for dimerization and stability of the calcium-binding protein S100B. *Biochemistry*, **41**, 3637–3646.
- Folkman, L. *et al.* (2016) EASE-MM: sequence-based prediction of mutation-induced stability changes with feature-based multiple models. *J. Mol. Biol.*, **428**, 1394–1405.
- Giollo, M. *et al.* (2014) NeEMO: a method using residue interaction networks to improve prediction of protein stability upon mutation. *BMC Genomics*, **15**, S7.
- Gribenko, A.V. and Makhatazde, G.I. (2007) Role of the charge-charge interactions in defining stability and halophilicity of the CspB proteins. *J. Mol. Biol.*, **366**, 842–856.
- Guerois, R. *et al.* (2002) Predicting changes in the stability of proteins and protein complexes: a study of more than 1000 mutations. *J. Mol. Biol.*, **320**, 369–387.
- Heijmans, R. (1999) When does the expectation of a ratio equal the ratio of expectations? *Stat. Papers*, **40**, 107–115.
- Huang, L.T. *et al.* (2007) iPTREE-STAB: interpretable decision tree based method for predicting protein stability changes upon mutations. *Bioinformatics*, **23**, 1292–1293.
- Keeler, C. *et al.* (2009) Contribution of individual histidines to the global stability of human prolactin. *Protein Sci.*, **18**, 909–920.
- Kumar, M.D. *et al.* (2006) ProTherm and ProNIT: thermodynamic databases for proteins and protein-nucleic acid interactions. *Nucleic Acids Res. (Database Issue)*, **34**, D204–D206.
- Laimer, J. *et al.* (2016) MAESTROweb: a web server for structure-based protein stability prediction. *Bioinformatics*, **32**, 1414–1416.
- Masso, M. and Vaisman, I. (2008) Accurate prediction of stability changes in protein mutants by combining machine learning with structure based computational mutagenesis. *Bioinformatics*, **24**, 2002–2009.
- Parthiban, V. *et al.* (2006) CUPSAT: prediction of protein stability upon point mutations. *Nucleic Acids Res.*, **34**, 239–242.
- Perl, D. and Schmid, F.X. (2001) Electrostatic stabilization of a thermophilic cold shock protein. *J. Mol. Biol.*, **313**, 343–357.
- Pires, D.E. *et al.* (2014) mCSM: predicting the effects of mutations in proteins using graph-based signatures. *Bioinformatics*, **30**, 335–342.
- Pires, D.E. *et al.* (2014b) DUET: a server for predicting effects of mutations on protein stability using an integrated computational approach. *Nucleic Acids Res.*, **42**, 314–319.
- Pucci, F. *et al.* (2017) SCooP: an accurate and fast predictor of protein stability curves as a function of temperature. *Bioinformatics*, **33**, 3415–3422.
- Savojarco, C. *et al.* (2016) INPS-MD: a web server to predict stability of protein variants from sequence and structure. *Bioinformatics*, **32**, 2542–2544.
- Teng, S. *et al.* (2010) Sequence feature-based prediction of protein stability changes upon amino acid substitutions. *BMC Genomics*, **11**, S5.
- Topham, C.M. *et al.* (1997) Prediction of the stability of protein mutants based on structural environment-dependent amino acid substitution and propensity tables. *Protein Eng.*, **10**, 7–21.
- Wainreb, G. *et al.* (2011) Protein stability: a single recorded mutation aids in predicting the effects of other mutations in the same amino acid site. *Bioinformatics*, **27**, 3286–3292.
- Worth, C.L. *et al.* (2011) SDM—a server for predicting effects of mutations on protein stability and malfunction. *Nucleic Acids Res.*, **39**, 215–222.
- Yang, Y. *et al.* (2018) PON-tstab: protein variant stability predictor. importance of training data quality. *Int. J. Mol. Sci.*, **19**, 1009.
- Yin, S. *et al.* (2007) Eris: an automated estimator of protein stability. *Nat. Methods*, **4**, 466–467.
- Zhou, H. and Zhou, Y. (2002) Distance-scaled, finite ideal-gas reference state improves structure-derived potentials of mean force for structure selection and stability prediction. *Protein Sci.*, **11**, 2714–2726.